Laidlaw Research Essay:

Comparative analysis of total and partial body irradiation in nonhuman primates over 60 days in urine, serum, and saliva

Alfonso Chan [1 2], Emma Kosowski [2], Denise Nishita [3], James Bakke [3], Janet Gahagen [3], Shweta Kapur [3], Polly Chang [3], Evagelia C. Laiakis [2]

[1]Laidlaw Scholars Programme, [2]Georgetown University Medical Center, [3]SRI International

Essay written by Alfonso "Rico" Chan 08/15/2025

ABSTRACT:

The prevalence of radiological incidents throughout history makes emergency preparedness an imperative component of national security. Assessment of exposed individuals and timely medical management will prove a critical capability in response to radiological or nuclear incidents. While previous works have investigated acute radiation exposure through total body irradiation of mammalian models, realistic environments will introduce shielding from radiation sources with differential dose compositions. Radiation shielding may alter biodosimetric signatures resulting in underestimation of biological dose and inappropriate medical management.

We previously developed biofluid metabolomic signatures from nonhuman primates (NHPs) (up to 60 days) exposed to an acute total body gamma radiation dose of 4 Gy. In the present study, male and female NHPs were either total body irradiated (TBI) with 5.5 Gy or partial body irradiated (PBI) with 5.5 Gy and 5% bone marrow shielding. Urine, serum, and saliva were collected pre-exposure and at specific timepoints throughout the 60 days after irradiation. Untargeted metabolomic analysis via liquid chromatography high-resolution time-of-flight mass spectrometry (LC-MS) was performed on all three biofluids. Previously identified TBI biomarkers were applied to compare PBI responses in the present cohort. Data were normalized, log transformed, and Pareto scaled for multivariate data analysis. Criteria involved fold changes, p-value determination, principal component analysis (PCA), heatmaps, and receiver operating characteristic curve (ROC) construction. Results are mixed with most TBI biomarkers failing to maintain diagnostic applicability in time-dependent circumstances. Results suggest saliva biomarkers exhibit similar behavior irrespective of shielding and could be used as radiation specific signatures. Other biomarker analyses show a shift in responses between TBI

and PBI indicative of organ specific origin (e.g. bone marrow). Preliminary analysis supports renal and hematopoietic system sensitivity to radiation shielding. Analysis is ongoing and will incorporate additional parameters (sex, weight, hematology, etc.) to enrich conclusions.

INTRODUCTION:

From foreign adversaries to domestic terrorists, the possibility of radiological incidents has long loomed over humanity. Infamous events like Hiroshima, Chernobyl, and the SL-1 US Army reactor explosion demonstrate how radiological exposure can impact civilians, first responders, and military personnel alike. Robust mitigation, triage, and treatment mechanisms will instill faith in future generations' emergency preparedness and minimize the magnitude of future tragedies.

Efforts to build better response mechanisms to acute radiation exposures are primarily led by medical researchers. As human experimentation in this field is deeply unethical, researchers have pursued alternative models to investigate physiological responses to acute radiation exposure. Robust characterization of animal models is imperative to the advancement of radiation exposure response capabilities. *MacVittie et al.* (2019) demonstrate the applicability of rhesus macaques toward modeling gastrointestinal (GI) and hematopoietic acute radiation syndromes, two drivers of patient outcomes following radiation exposure. To first address clinical research questions, however, accurate dose severity detection and classification methods are necessary.

Biomarkers of acute radiation exposure are not only relevant to public health responses, but also complement improved understanding of mechanisms governing mammalian response to radiation. Biomarkers involving large quantities of small molecules (also known as metabolomic

biomarkers), have already been developed from acute radiation exposures of mice and NHPs. *Pannkuk et al.* (2019) have successfully applied global liquid chromatography-mass spectrometry (LC-MS) metabolomics in NHP urine and saliva to differentiate time after 4 Gy TBI. *Laiakis et al.* (2019) similarly characterized NHP saliva following 4 Gy TBI and identified long-term metabolites (primarily nucleotides and amino acids) with strong diagnostic potential.

Symptoms resulting from high human radiation doses (0.7 Gy) are formally referred to as acute radiation syndrome (ARS) and include three significant presentations: hematopoietic, gastrointestinal, and cardiovascular/central nervous system syndromes (CDC 2024, *López et al.* 2011). As presentation of radiation exposure is dependent upon the biological systems affected and the extent of their exposure, shielding of central organs is a primary concern for characterization and clinical management. Bone marrow shielding exemplifies a PBI method that may inform researchers regarding the hematopoietic system's relevance in radiation response. Other PBI methods divide models into regions (e.g., upper and lower body) for selective irradiation.

Pannkuk et al. (2024) presented an investigation of PBI in murine models using NHP TBI biomarkers; results suggested that metabolomic biomarkers, including low molecular weight molecules, would hold between PBI mice with upper and lower body shielding. The present study applies pre-existing TBI biomarkers to LC-MS data collected from NHP biofluids (saliva, urine, and serum) following 5.5 Gy TBI and PBI. Results suggest TBI biomarkers may be applicable to serum and urine after an initial acute radiation exposure, but diminish in accuracy as time progresses. Results support both hematopoietic and GI system responses to acute radiation exposure with PBI eliciting differential response activity after 1 week post-exposure. Furthermore, pre-determined saliva biomarkers were found to maintain diagnostic significance

between TBI and PBI cohorts. Future works ought to develop generalized radiation, PBI, and TBI biomarkers to differentiate between shielding influence and maintain applicability. Analysis is ongoing and the present study represents a preliminary review of observations.

METHODS:

Management and treatment of NHPs detailed in the present paragraph were conducted at Charles River Laboratory. Nine total Indian Rhesus Macaque monkeys (3-21 y/o) were either treated with a placebo (2 sham), exposed to 5.5 Gy gamma irradiation (4 TBI), or exposed to 5.5 Gy gamma irradiation with ~5% bone marrow sparing (3 TBI) (Fig. 1A). PBI with 5% bone marrow shielding was achieved with cerrobend structures over the lower legs to protect the tibia, ankles, and feet. The actual measured dose for all irradiations was closer to 5.6 Gy according to Farmer ionization chamber measurements. Irradiations were performed using a ^{60}Co irradiator at ~0.43 Gy/min. Four NHPs were noted to have deteriorated and were humanely euthanized. Saliva, urine, and serum were collected as available at times -7, -3, 1, 3, 5, 7, 14, 21, 28, and 60 days relative to the time of irradiation.

All preparations of biofluids for LC-MS were designed and executed by E. Kosowski as outlined in *Kosowski et al.* (2024). LC-MS provides three major datapoints: abundance (relative concentrations of each species), retention time (the separation of each species due to interactions with the column), and fragmentation (patterns in remaining species after ionization and breaking covalent bonds). LC-MS was untargeted, meaning all ionized compounds (both positive and negative) were recorded without application of a mass-specific filter. All LC-MS data were filtered and normalized to prevent outlying abundances from skewing downstream analysis.

Biofluid LC-MS data were screened for molecular ions and retention times that match the databases and previously identified biomarkers (*Kosowski et al.* 2024; *Laiakis et al.* 2019; *Pannkuk et al.* 2015, 2016, 2018, 2018, 2019, 2024). Matches with reasonable variation were exported into biomarker lists for each biofluid and validated with Progenesis QI. A list of included biomarkers for serum, urine, and saliva is depicted in Table 1. Biomarkers that were not identified manually were further screened using Progenesis QI and the databases HMDB, METLIN, and Lipid Blast.

Post-metabolic fingerprinting analysis was performed on both TBI biomarkers and untargeted outputs using MetaboAnalyst 6.0 statistical analysis [one factor] and biomarker analysis functions. A low-variance filter (IQR 40%) was applied for untargeted datasets exceeding 1000 variables. Missing values were accounted for with left-censored data estimation at ⅕ of the minimum positive value. Data were log transformed and Pareto scaled.

Analyses performed included analysis of variance (ANOVA) ($p = 0.05$), principal component analysis (PCA), partial least squares-discriminant analysis (PLS-DA), and heatmap generation of both PBI and TBI cohorts. Normalized abundances of metabolic biomarkers were log-scaled, compared, and screened for significance with the software GraphPad Prism v.10.5. Experimental groups were divided into before day 7 (including data from day 7) and after day 7 up to day 60. Day 3 pre-irradiation samples were included in both timepoint analyses. Day 7 pre-irradiation was not used due to significant variance between the considered samples.

Diagnostic capabilities were evaluated through ROC curves and reporting area under the curve (AUC). Regarding ROC curves, PBI or TBI vs. pre analysis for each biofluid was performed alongside direct PBI-TBI comparison.

RESULTS AND DISCUSSION:

While PCA aims to describe variance between datapoints and groups, PCA plots for biomarkers were generally cluttered with no self-evident trends (Fig. 2). This outcome was expected, given that the samples were not separated by sex, weight, and other relevant parameters. The current PCA 2D plots assist in visualizing multivariate data and rule out extreme outliers. PLS-DA generates a model for differentiation between populations. PLS-DA results for all biomarkers were either insignificant or overfit the data (Fig. 3). Based on these results, incorporation of additional sample information is necessary for PLS-DA delineation of group classifications.

ANOVA of untargeted ions generally yielded significant results at both a higher frequency and volume compared to TBI biomarker ANOVA, as depicted by urine samples in (Fig. 4). While this outcome is expected due to the sheer holistic volume of untargeted ions, the high frequency of outlying ions suggests additional markers may exist for PBI response. Future analysis will identify the foremost ions and re-evaluate data with their known identities. Metabolomic fingerprinting of identified ions will support physiological explanations for the observed radiation response.

Although both PBI and TBI results reflect renal system response, deviation between shielding cohorts suggests PBI induces a different response magnitude. TBI ROC curve AUCs remained close to 1.0 in the first week and slightly decreased in the following weeks, although AUC > 0.9 indicates an excellent classification model (Fig. 5A). PBI ROC curves, however, displayed weaker AUCs (around 0.8) during week 1, although an AUC > 0.8 indicates a good classification model and is used as a cut-off in radiation biodosimetry through metabolomics (Fig. 5B). PBI ROC curve AUCs fell as low as 0.782 after week 1, suggesting urinary TBI

biomarkers lose diagnostic applicability at timepoints greater than 1 week (Fig. 5B). The diagnostic signal could be increased with the addition of other biomarkers that are more prevalent after 1 week. ROC curve pattern similarities between PBI and TBI reinforce the renal system as the primary contributor to the observed metabolic response. Lowered PBI ROC curve AUC following week 1 is likely due to the extent of radiation damage affecting the renal system, thus producing a less drastic response.

Renal system response in both PBI and TBI cohorts is further explained by metabolite analysis. Both 4-pyridoxic acid and xanthurenic acid normalized abundances were observed to change throughout the first weeks following exposure, with heightened responses at day 1 (Fig. 5D, 5E). 4-Pyridoxic acid is a methylpyridine catabolic product of vitamin B6 commonly excreted in urine. Results were expected, as anemia was recorded in the NHP population within the first week. It should be noted that TBI 4-pyridoxic acid normalized abundances were higher than those of PBI samples (Fig. 5D). Further analysis of clinical reports will be necessary to detail the affected pathway.

Similar patterns were observed with xanthurenic acid, as normalized abundance for both PBI and TBI peaked 1 day post-irradiation; elevated xanthurenic acid normalized abundance persisted following day 1 (Fig. 5E). Xanthurenic acid is a quinoline carboxylic acid present within cell membranes and found in blood, feces, urine, and epidermis tissues. Xanthurenic acid serves as an enzyme substrate during Tryptophan catabolism, further reinforcing the presence of a renal system response to acute radiation. Evaluation of tryptophan levels across clinical reports will elucidate the underlying mechanisms behind observations.

Serum ROC curves of both PBI and TBI groups depict changing AUC indicative of a differential hematopoietic response (Fig. 6A, 6B). TBI ROC curves depict AUC > 0.7 until day

60, while PBI AUC falls below 0.7 on day 21 (Fig. 6A, 6B). Serum TBI biomarkers, therefore, fail in diagnostic capability between the 2 and 3-week mark. This result is expected as bone marrow sparing induced differential damage to hematopoietic mechanisms, resulting in a dampened response.

Radiation quality's impact on the hematopoietic system is further supported by heightened day 1 acetylcarnitine in the PBI cohort (Fig. 6C). Acetylcarnitine facilitates acetyl-CoA movement into matrices of mammalian mitochondria during fatty acid beta oxidation and exhibits widespread presentation in biofluids. Analysis of hematology reports will provide a stronger description of hematopoietic progression and the impacts of PBI. Additionally, stronger insights regarding acetylcarnitine's role in the hematopoietic system may be found.

Saliva preliminary analysis via ROC curves showed little to no discrepancies between PBI and TBI cohorts, meaning pre-determined saliva biomarkers may be applied independent of shielding effects (Fig. 7). Untargeted heatmaps display general metabolic trends across PBI and TBI populations that may support biomarkers that distinguish radiation shielding (Fig. 8). Besides strong preliminary evidence of biomarker determination, robust conclusions were not expected for saliva, as the pre-existing TBI biomarkers were intended for pre- and post-week 1 datasets. Our analysis mixed all biomarkers independent of initial intention, thus introducing uncertainty in the results. Ongoing efforts ought to account for time-specific biomarkers and repeat analysis.

CONCLUSION:

Saliva, urine, and serum of NHPs following TBI and PBI with 5% bone marrow sparing were recorded via liquid chromatography high-resolution time-of-flight mass spectrometry.

Multivariate analysis was performed to evaluate the efficacy of TBI biomarkers on PBI populations. Results are mixed, with some TBI biomarkers providing viable diagnostic capability within week 1 and falling short at later time points. Preliminary analysis instills confidence in results as processes fundamental to acute radiation exposure are observed with perturbations between PBI and TBI cohorts. Analysis is ongoing and will incorporate relevant parameters like sex, weight, and clinical reports to better explain observed trends. Untargeted metabolomics of all three biofluids supports future endeavors to identify PBI biomarkers. Comparative analysis and identification of biomarkers will fill a gap in radiological medical response capabilities.

REFLECTION ON SUMMER RESEARCH:

I am privileged to have completed a research-intensive summer surrounded by peers and mentors supportive of my development. I began my summer at Lawrence Livermore National Laboratory (LLNL) in Livermore, California, where I investigated groundwater organic molecule sorption to mineral surfaces as a model for carbon sequestration. As I had little experience in environmental science and geochemistry, working under Dr. Mavrik Zavarin and presenting my findings to leading professionals proved a challenge. I found, however, that my background in physics and chemistry has equipped me with the underlying principles necessary to understand foreign fields from the ground up. After reviewing the mechanics behind sorption processes and modeling trends relevant to our objectives, I found that my contributions provided a fresh perspective, even though I lacked a shared background with my team. Working on a project with minimal experience in relevant fields proved incredibly worthwhile to my development as a team-based scientist.

My time at LLNL was much more than the work described above, however. From meeting cross-disciplinary researchers to touring one-of-a-kind facilities, my understanding of STEM as a professional field was deeply enriched. Additionally, learning alongside a cohort of similarly driven, aspiring scientists fostered an environment that drove my thirst for every opportunity available at LLNL. Going forward, I will carry my time at LLNL close to heart and perpetuate the flame of curiosity enkindled by my peers and mentors.

After completing my work at LLNL, I returned to Washington, D.C. to begin my Laidlaw summer research project under Prof. Evagelia Laiakis at Georgetown University Medical Center. Although I had previously processed rudimentary mass spec data in my organic chemistry lab, metabolomics via LC-MS was completely different. In response to the high volume of ion abundances, I learned to compare spectra against databases via ProgenesisQI. To process biomarkers and untargeted ions, I also learned how to utilize MetaboAnalyst 6.0, an R graphic user interface with multivariate analysis functions.

Looking back, I wish I had spent more time diving into relevant biostatistics for multivariate analysis. While I spent substantial amounts of time reading past literature, figures, and relevant information, I also constructed assumptions regarding what my data would look like. As I obtained results, holding onto my preconceived notions led me astray in properly interpreting my findings. Going forward, I will learn new methods without underlying assumptions on how my data would look and rather build a strong foundational understanding to be later applied.

I ought to note that data began making sense only after compiling all findings in an organized manner. For example, interpreting ROC curves alone would not have allowed for effective comparison over time between PBI and TBI samples. This demonstrates the absolute

necessity for organization and efficient note-taking, as errors may easily propagate downstream and analysis can be lost amidst the high volume of results.

Learning more about the chemistry and statistics behind biomarker identification proved incredibly fulfilling. Before my Laidlaw summer research project, I had never considered the extent of testing required to produce robust clinical tests. I particularly enjoyed looking into biochemical pathways to explain my findings and anticipate more in-depth research of such mechanisms.

ACKNOWLEDGEMENTS:

This work was supported by the Laidlaw Scholars Programme, Georgetown University Center for Research and Fellowship, and National Institutes of Health (National Institute of Allergy and Infectious Diseases) grant U01AI148307 (P.I.'s Evagelia C. Laiakis and Frederic Zenhausern). This project has been funded in whole or in part with Federal funds from the National Institute of Allergy and Infectious Diseases, National Institutes of Health, Department of Health and Human Services, under Contract No. HHSN272201500013I awarded to SRI International. The project described above was also supported by Award Number P30 CA051008 (P.I. Louis Weiner) from the National Cancer Institute. The content is solely the responsibility of the authors and does not necessarily represent the official views of the National Institute of Allergy and Infectious Diseases or the National Institutes of Health. I would like to particularly thank Professor Evagelia Laiakis for her continued support, patience, guidance, and mentorship throughout my Laidlaw research summer.

REFERENCES:

Acute Radiation Syndrome: Information for Clinicians | Radiation Emergencies. (2024, April 23). Center for Disease Control**.** Retrieved August 14, 2025, from https://www.cdc.gov/radiation-emergencies/hcp/clinical-guidance/ars.html

Kosowski, E., Olson, J. D., Gardin, J., Schaaf, G. W., Nishita, D., Authier, S., Chang, P., Brenner, D. J., Fornace, A. J., Jr, Cline, J. M., & Laiakis, E. C. (2024). Long-term radiation signal persistence in urine and blood: A two-year analysis in non-human primates exposed to a 4 Gy total-body gamma-radiation dose. Radiation Research. Advance online publication. https://doi.org/10.1667/RADE-23-00261.1

Laiakis, E. C., Nishita, D., Bujold, K., Jayatilake, M. M., Bakke, J., Gahagen, J., Authier, S., Chang, P., & Fornace, A. J., Jr (2019). Salivary metabolomics of total body irradiated nonhuman primates reveals long-term normal tissue responses to radiation. International Journal of Radiation Oncology, Biology, Physics, 105(4), 843–851. https://doi.org/10.1016/j.ijrobp.2019.07.017

López, M., & Martín, M. (2011). Medical management of the acute radiation syndrome. Reports of Practical Oncology and Radiotherapy, 16(4), 138–146. https://doi.org/10.1016/j.rpor.2011.05.001

MacVittie, T. J., Farese, A. M., & Jackson, W., 3rd (2015). The hematopoietic syndrome of the acute radiation syndrome in rhesus macaques: A systematic review of the lethal dose response relationship. Health Physics, 109(5), 342–366. https://doi.org/10.1097/HP.0000000000000352

MacVittie, T. J., Farese, A. M., Parker, G. A., Jackson, W., 3rd, Booth, C., Tudor, G. L., Hankey, K. G., & Potten, C. S. (2019). The gastrointestinal subsyndrome of the acute radiation syndrome in rhesus macaques: A systematic review of the lethal dose-response relationship with and without medical management. Health Physics, 116(3), 305–338. https://doi.org/10.1097/HP.0000000000000903

Pannkuk, E. L., Laiakis, E. C., Authier, S., Wong, K., & Fornace, A. J., Jr (2015). Global metabolomic identification of long-term dose-dependent urinary biomarkers in nonhuman primates exposed to ionizing radiation. Radiation Research, 184(2), 121–133. https://doi.org/10.1667/rr14091.1

Pannkuk, E. L., Laiakis, E. C., Mak, T. D., Astarita, G., Authier, S., Wong, K., & Fornace, A. J., Jr (2016). A lipidomic and metabolomic serum signature from nonhuman primates exposed to ionizing radiation. Metabolomics, 12(5), 80. https://doi.org/10.1007/s11306-016-1010-0

Pannkuk, E. L., Laiakis, E. C., Fornace, A. J., Jr, Fatanmi, O. O., & Singh, V. K. (2018). A metabolomic serum signature from nonhuman primates treated with a radiation countermeasure, gamma-tocotrienol, and exposed to ionizing radiation. Health Physics, 115(1), 3–11. https://doi.org/10.1097/HP.0000000000000776

Pannkuk, E. L., Laiakis, E. C., Garcia, M., Fornace, A. J., Jr, & Singh, V. K. (2018). Nonhuman primates with acute radiation syndrome: Results from a global serum metabolomics study after 7.2 Gy total-body irradiation. Radiation Research, 190(6), 576–583. https://doi.org/10.1667/RR15167.1

Pannkuk, E. L., Laiakis, E. C., Gill, K., Jain, S. K., Mehta, K. Y., Nishita, D., Bujold, K., Bakke, J., Gahagen, J., Authier, S., Chang, P., & Fornace, A. J., Jr (2019). Liquid chromatography–mass spectrometry-based metabolomics of nonhuman primates after 4 Gy total body radiation exposure: Global effects and targeted panels. Journal of Proteome Research, 18(5), 2260–2269. https://doi.org/10.1021/acs.jproteome.9b00101

Pannkuk, E. L., Laiakis, E. C., Garty, G., Bansal, S., Jayatilake, M. M., Tan, Y., Ponnaiya, B., Wu, X., Amundson, S. A., Brenner, D. J., & Fornace, A. J., Jr (2024). Impact of partial body shielding from very high dose rates on untargeted metabolomics in biodosimetry. ACS Omega, 9(32), 35182–35196. https://doi.org/10.1021/acsomega.4c05688

Satyamitra, M. M., DiCarlo, A. L., Hollingsworth, B. A., Winters, T. A., & Taliaferro, L. P. (2022). Development of biomarkers for radiation biodosimetry and medical countermeasures research: Current status, utility, and regulatory pathways. Radiation Research, 197(5), 514–532. https://doi.org/10.1667/RADE-21-00157.1

INDEX:

Table 1: List of pre-determined metabolite biomarkers for TBI exposure applied in this study. +/- indicates cation/anion. Metabolites sourced from *Kosowski et al.* 2024; *Laiakis et al.* 2019; *Pannkuk et al.* 2015, 2016, 2018, 2018, 2019, 2024.

Urine	Saliva	Serum
Cortisone (+)	Propionylcarnitine (pos)	Carnitine (+)
Kynurenate (+)	L-Citrulline (+)	Acetylcarnitine (+)
Propionylcarnitine (+)	Guanosine (+)	LysoPC (14:0)a (+)
Cortisol (+)	L-Leucine/Isoleucine (-)	MG (18:2)a (+)
L-Cartinine (+)	Xanthine (-)	3-Dehydroxycarnitine (+)
Xanthurenate (+)	Sebacate (-)	Propionylcarnitine (+)
7-Methylguanine (+)	Hypoxanthine (-)	Arginine (+)
L-Acetylcarnitine (+)	Glutamate (-)	Oleamide (+)
Isobutyryl-L-Carnitine (+)	Glutarate (-)	Taurine (-)
7-methylguanine (+)	L-Histidine (-)	Methylmalonic acid (-)
Xanthurenate (-)	L-Phenylalanine (-)	
Taurine (-)		
cis-Aconitate (-)		
Malate (-)		
Urate (-)		
L-Alanine (-)		
Pantothenate (-)		
Azelaate (-)		
Hexanoylglycine (-)		
Oxoglutarate (-)		
Citrate (-)		
Xanthine (-)		
Fumarate (-)		
Methylmalonate (-)		
Xanthosine (-)		
Creatine (-)		
Hypoxanthine (+)		
4-Pyridoxicate (-)		

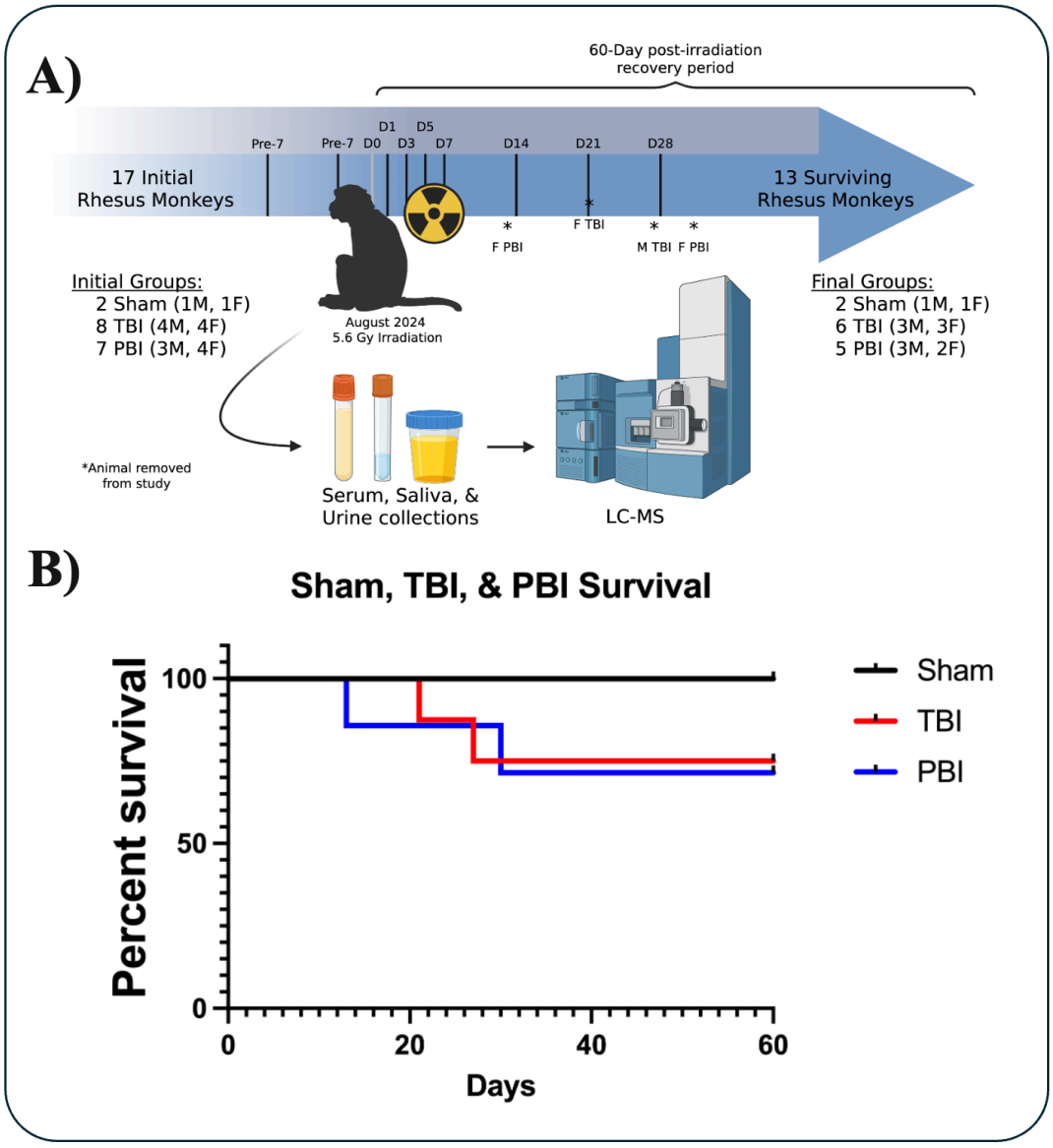

Figure 1: A) Experimental setup and sample collection times. Three NHPs met euthanasia criteria, four were removed from study. B) Kaplan Meier curve depicts survival rates for all cohorts over 60-day post-irradiation period. Graphics created with BioRender.com.

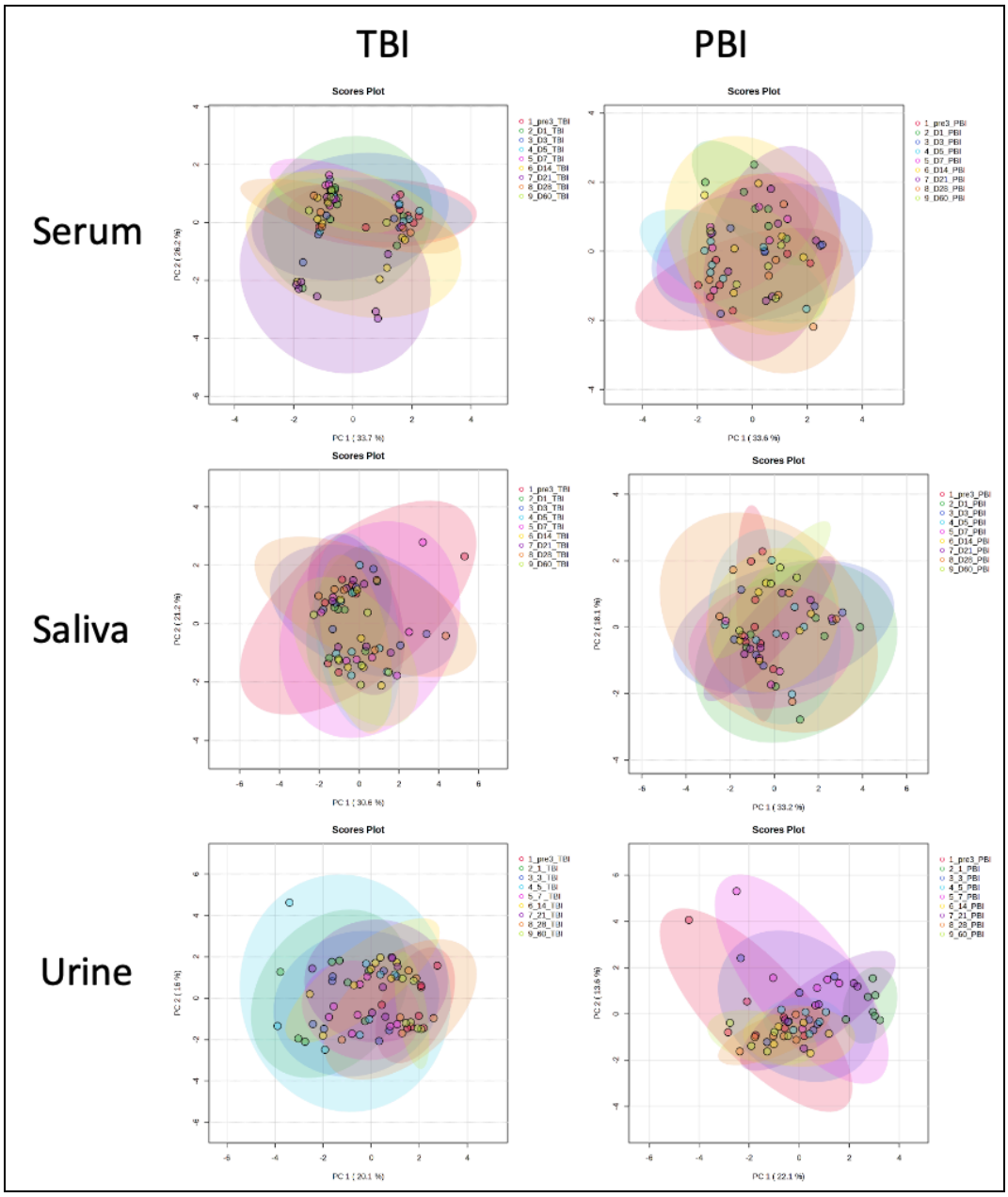

Figure 2: PCA depicting abundances collected from all cohorts serum, saliva, and urine samples. All abundances were normalized, Pareto scaled, and log-transformed.

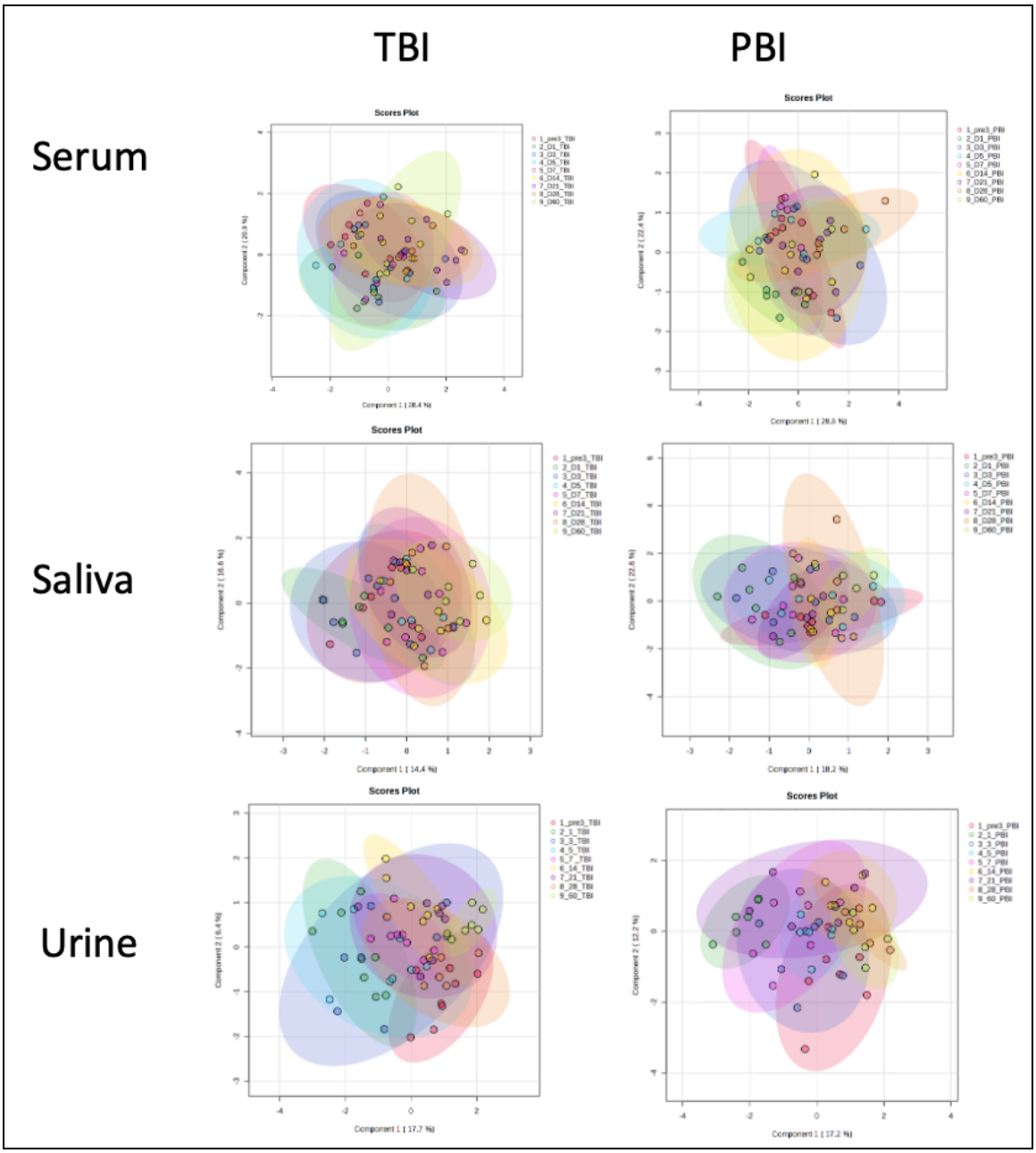

Figure 3: PLS-DA depicting models for delineation between sample times for serum, saliva, and urine. All abundances were normalized, Pareto scaled, and log-transformed. None of the above models were significant or did not overfit data.

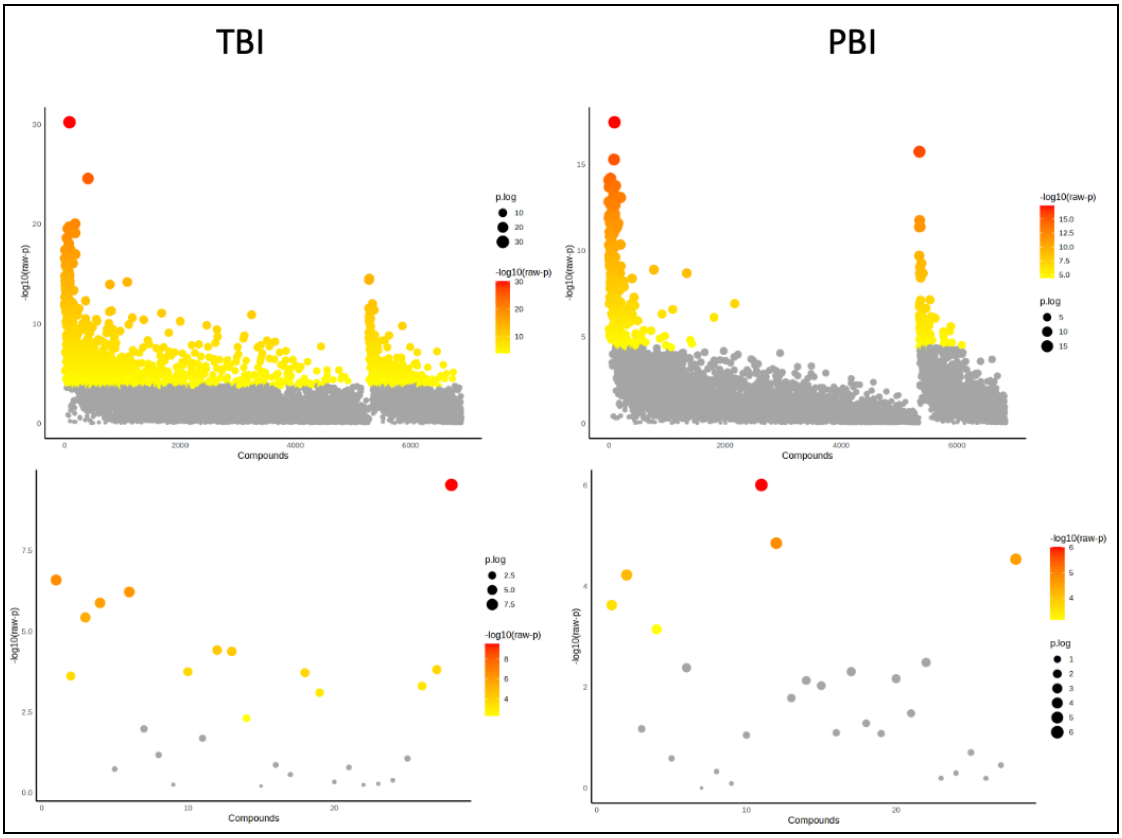

Figure 4: ANOVA comparison of both targeted (below) and untargeted (above) urine samples over entire 60 day period (p=0.05). ANOVA also includes pre-irradiation day 3 samples.

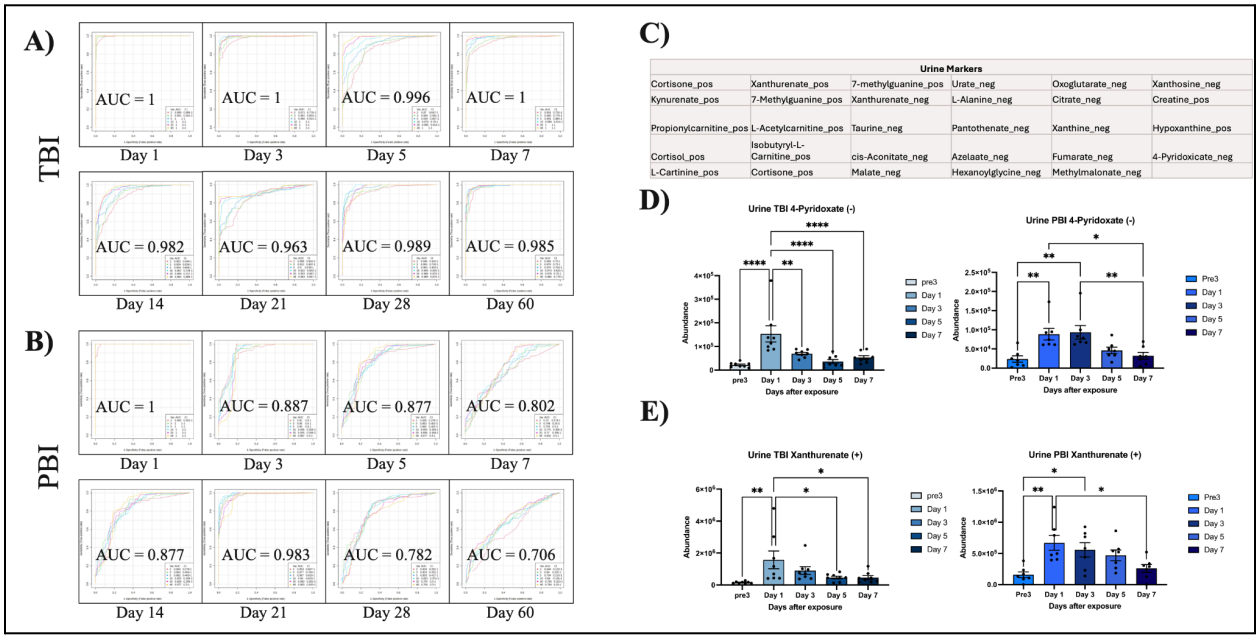

Figure 5: A) TBI and **B)** PBI ROC curves of urine metabolic response throughout 60-day post-irradiation period. ROC curves built using pre-determined TBI biomarkers. **C)** List of all urine TBI markers sourced from literature and applied to both cohorts. **D)** Bar graph comparison of 4-Pyridoxicate (-) and **E)** xanthurenate (+) abundances up to one week post-irradiation. All abundances normalized.

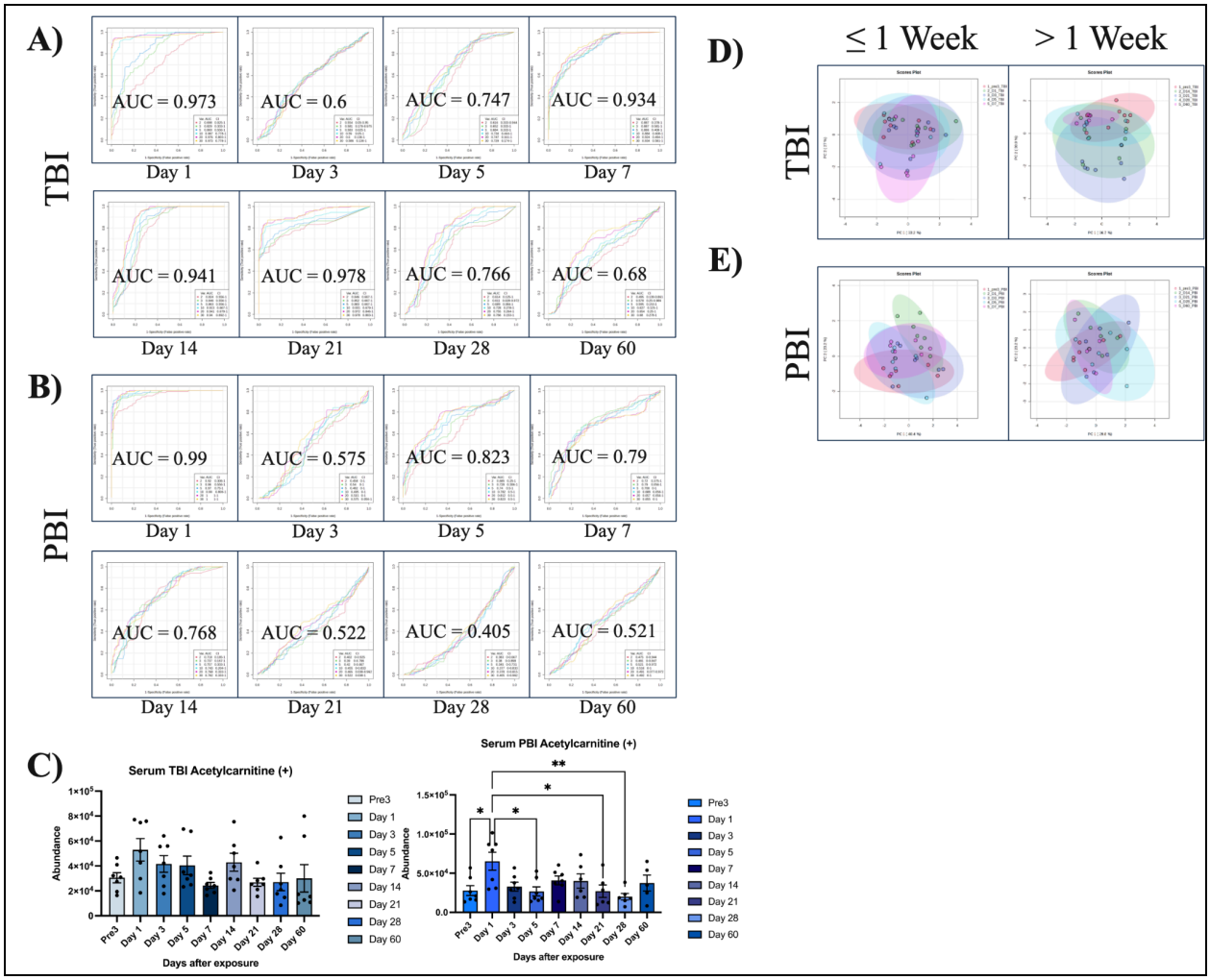

Figure 6: A) TBI and **B)** PBI ROC curves of serum metabolic response throughout 60-day post-irradiation period. ROC curves built using pre-determined TBI biomarkers. **C)** Bar graph comparisons of Acetylcarnitine (+) abundance through 60 days. **D)** PCA of serum sourced from TBI and **E)** PBI cohorts separated by 1 week mark. Pre3 included in all PCA analyses. All abundances normalized.

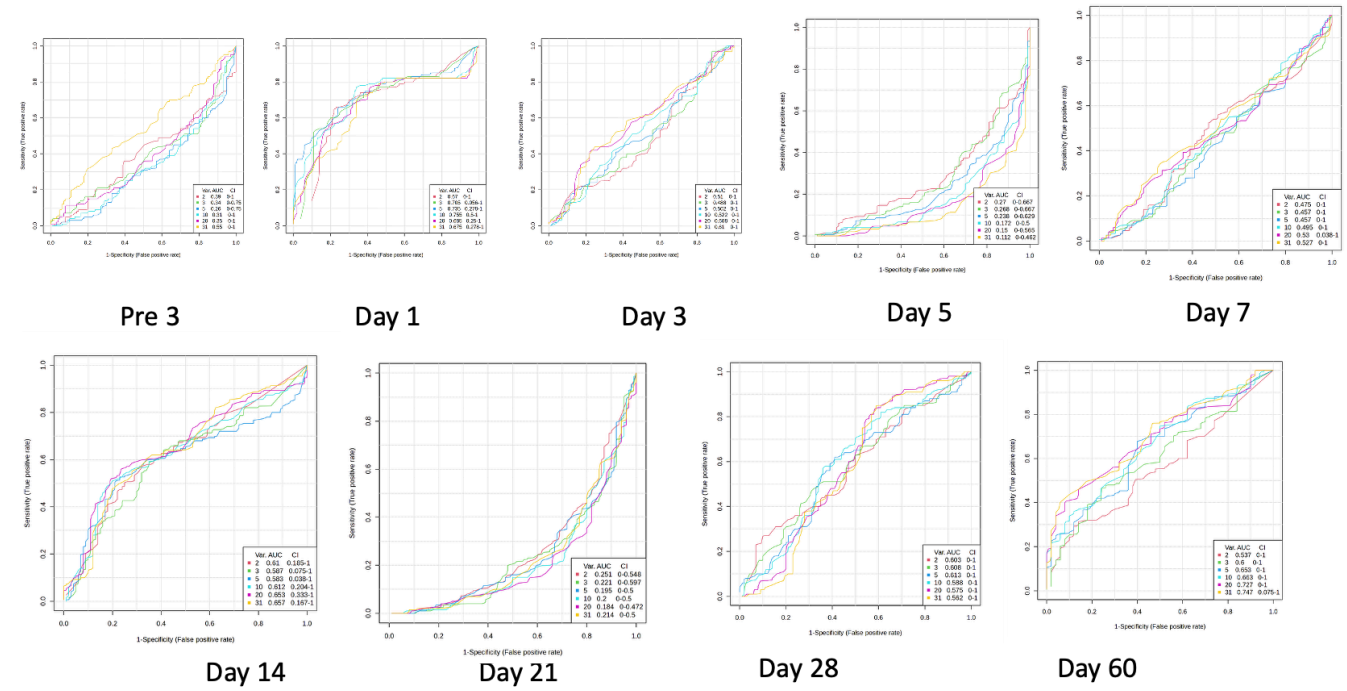

Figure 7: ROC curve analysis between PBI and TBI saliva samples. Note AUC is consistently low.

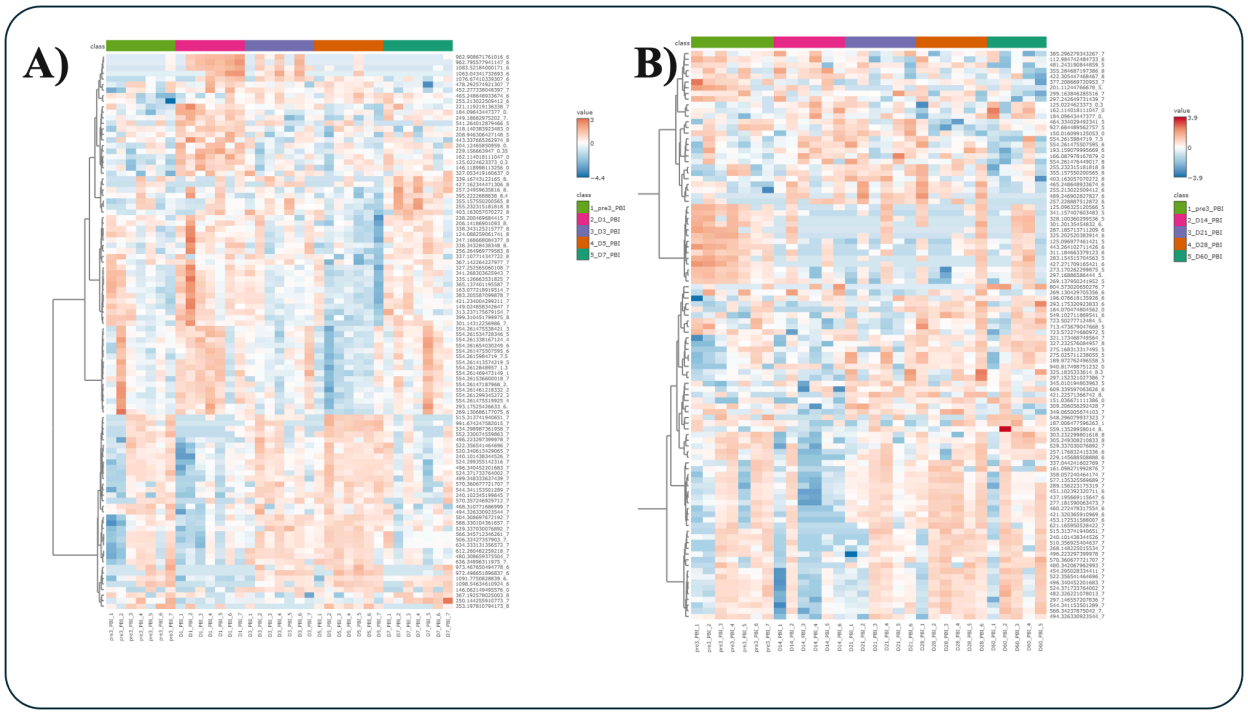

Figure 8: A) Untargeted heatmaps featuring top 100 (+) and (-) measurements for times ≤ 1 week and **B)** > 1 week. Both heatmaps include pre-irradiation samples. Heatmaps depict changes in ion abundances for each cohort compared to day 3 pre-irradiation. All abundances normalized.